nature communications

Article

https://doi.org/10.1038/s41467-025-59818-8

# Engineering anti-BCMA CAR T cells for enhancing myeloma killing efficacy via apoptosis regulation

Received: 21 November 2023

Accepted: 6 May 2025

Published online: 19 May 2025

Check for updates

Thomas Kimman[1,8], Marta Cuenca[1,8], Ralph G. Tieland[1], Dedeke Rockx-Brouwer[1], Jasmijn Janssen[2], Benjamin Motais[1,3], Anne Slomp[1], Corine Pleijte[1], Sabine Heijhuurs[1], Angelo D. Meringa[1], Wendy Boschloo[1], Douwe MT Bosma[1], Sanne Kroos[1], Vania lo Presti[1,4], Joost P. G. Sluijter[2,5], Stefan Nierkens[1,4,6], Niels Bovenschen[1,5,7], Jürgen Kuball[1,3,5], Alain van Mil[2,5], Monique C. Minnema[3,5], Zsolt Sebestyén[1,5] & Victor Peperzak[1,5]

Clinical responses with chimeric antigen receptor (CAR) T cells are encouraging, but primary resistance and relapse after therapy prevent durable remission in many patients with cancer, with apoptosis resistance in cancer cells that limits killing by CAR T cells being a potential cause. Here we aim to boost tumor cell apoptosis induced by CAR T cells and find that anti-B cell maturation antigen (BCMA) CAR T cells over-expressing a granzyme B-NOXA fusion protein show improved killing of multiple myeloma (MM) cells in vitro and in xenograft mouse models in vivo. Mechanistically, such an enhancement is mediated by localizing NOXA to cytotoxic granules that are released into cancer cells upon contact. In MM cells, inhibition of MCL-1, an anti-apoptotic factor, by its natural ligand NOXA effectively induces apoptosis. Our data thus show that endowing granzyme B-NOXA expression to CAR T cells improves their killing efficacy, thereby presenting a potential generalizable enhancement for CAR T-mediated anti-cancer immunity.

Recent clinical success of immunotherapy has made a colossal impact on the development of novel therapeutic approaches targeting cancer. Engineered T cell therapy is, together with the discovery of checkpoint inhibitors, one of the most promising types of anti-cancer immunotherapy where scientific efforts are accompanied with high investments by industry[1]. Despite their initial successes, clinical trials with engineered T cells, and specifically with chimeric antigen receptor (CAR) T cells, revealed two major weaknesses: (1) primary resistance upon treatment with anti-CD19 CAR T cells in chronic lymphocytic leukemia (CLL) and diffuse large B cell lymphoma (DLBCL), and (2) disease relapse after treatment with anti-CD19 CAR T cells for B cell acute lymphoblastic leukemia (B-ALL) or with anti-B cell maturation antigen (BCMA) CAR T cells for multiple myeloma (MM)[2,3]. Resolving these weaknesses could greatly increase the effectiveness and broad applicability of engineered T cell therapy against cancer.

Previously described limitations to successful CAR T cell therapy include antigen loss on cancer cells and failed CAR T cell expansion and persistence[4]. While multiple strategies have been considered to improve gene-engineered T cells, attempts to directly improve their killing capacity remain neglected[5]. If initial CAR T cell-directed killing of cancer cells can be improved, subsequent selection for antigen-negative cancer cells and CAR T cell persistence become less relevant.

[1]Center for Translational Immunology, University Medical Center Utrecht, Utrecht, Netherlands. [2]Department of Cardiology, University Medical Center Utrecht, Utrecht, Netherlands. [3]Department of Hematology, University Medical Centre Utrecht, Utrecht, Netherlands. [4]Blood and Marrow Transplantation Program, Princess Máxima Center for Pediatric Oncology, Utrecht, The Netherlands. [5]Utrecht University, Utrecht, Netherlands. [6]Princess Máxima Center for Pediatric Oncology, Utrecht, The Netherlands. [7]Department of Pathology, University Medical Centre Utrecht, Utrecht, Netherlands. [8]These authors contributed equally: Thomas Kimman, Marta Cuenca. e-mail: v.peperzak@umcutrecht.nl

There is ample evidence that CAR T cell-induced apoptosis is often suboptimal and that apoptosis resistance mechanisms limit effective responses to CAR T cell therapy in various B cell malignancies. For example, increased expression of pro-survival protein BCL-2 has been observed in B lymphoma cells that survive treatment with anti-CD19 CAR T cells and therefore entails a resistance mechanism that disables the natural killing machinery of CAR T cells[6]. In line with these findings it was shown using genome-wide CRISPR/Cas9 screening that loss of pro-apoptotic BCL-2 family protein NOXA in B lymphoma cells regulates resistance to CAR T cell therapy by impairing apoptosis of tumor cells[7]. Execution of target cell apoptosis can be mediated by the release of granzymes by CAR T cells or by engaging death receptors on targeted cancer cells. Interestingly, resistance mechanisms for both pathways have been described. Two separate studies used genome-wide CRISPR/Cas9 knock-out screens in B-ALL cells to reveal that death receptor TRAIL-R2 (TNFRSF10B), and downstream signaling molecules FADD, BID, and CASP8, mediate sensitivity to anti-CD19 CAR T cell killing[8,9]. In addition, we have recently shown that expression of granzyme B-inhibitor serpin B9 in DLBCL and CLL cells inhibits killing by anti-CD19 or anti-CD20 CAR T cells, thereby revealing another apoptosis resistance mechanism[10].

MM is characterized by the accumulation of malignant plasma cells within the bone marrow niche. Although advances in MM treatment resulted in improved patient survival it is still considered incurable due to the development of therapy resistance and relapse[11]. BCMA is currently the most extensively investigated target in MM and novel immunotherapeutic approaches targeting BCMA, including antibody-drug conjugates, bispecific antibodies and CAR T cells, yielded promising clinical results[12]. Complete response (CR) rates after anti-BCMA CAR T cell therapy in multiple myeloma (MM) are high (up to 80%). Still, nearly all patients eventually relapse, even those achieving minimal residual disease (MRD)-negative CR rates[13]. Pro-survival B cell lymphoma 2 (BCL-2) family proteins are potent inhibitors of programmed cell death and are often over-expressed in cancer cells. BCL-2 family member MCL-1 is overexpressed in many germinal center-derived malignancies, including MM, and inhibiting MCL-1 in MM cells has been shown to result in rapid cell death[14,15]. Furthermore, a clear correlation exists between high MCL-1 expression and increased mortality in MM[16]. Thus, targeting MCL-1 may be beneficial for the treatment of MM. However, we and others have shown that MCL-1 expression is important for survival of many healthy cells and tissues, and therefore a systemic MCL-1 inhibitor would generate severe side effects, precluding its use as a safe anti-cancer drug. BH3-only protein NOXA is a p53-inducible selective inhibitor of MCL-1 and associated with apoptosis induction in many forms of cancer, including MM[17,18]. Interestingly, it was reported that pharmacologically induced expression of NOXA sensitized cancer cells to CAR T cell-mediated killing[7]. These findings indicate that the level of NOXA expression in cancer cells may determine their sensitivity to CAR T cell-mediated killing.

Here, rather than bypassing specific apoptosis resistance mechanisms, such as those described above, we explore the possibility of directly enhancing the killing potential of CAR T cells. We reveal that high expression of MCL-1 in MM cells limits killing by anti-BCMA CAR T cells which can be overcome by arming the CAR T cells with pro-apoptotic NOXA, a natural MCL-1 inhibitor. While NOXA is effectively transferred into encountered cancer cells resulting in apoptosis, we show that viability of non-targeted healthy cells in the microenvironment, including myocardiocytes, as well as the CAR T cells themselves is unaffected. By enhancing CAR T cell killing efficacy using apoptotic cargo we expect to dampen primary resistance of cancer cells and reduce the chance of disease relapse.

## Results

Since MCL-1 controls MM cell survival, we examined if MCL-1 expression was enriched in MM cells that resist killing by anti-BCMA CAR T cells (Fig. 1A). Human MM cell lines NCI-H929 and L363 were co-cultured with anti-BCMA CAR T cells and intracellular MCL-1 protein expression was subsequently measured in viable MM cells. We found that MCL-1 expression was increased in surviving MM cells after co-culture with anti-BCMA CAR T cells compared to expression in MM cells cultured alone (Fig. 1B, C). Importantly, selection of MCL-1$^{hi}$ cells was not observed in the absence of therapeutic selection when MM cells were co-cultured with non-MM-targeting anti-CD19 CAR T cells (Fig. 1C). Since MCL-1 can be targeted with specific small molecule inhibitors we added MCL-1-inhibitor S63845 (MCL-1i) during co-culture of MM cells with anti-BCMA CAR T cells[19,20]. This resulted in improved killing of MM cells compared to co-culture with anti-BCMA CAR T cells alone (Fig. 1D, E), including for L363 MM cells that are relatively resistant to anti-BCMA CAR T cells. The difference in sensitivity to anti-BCMA CAR T cells may in part be due to the level of BCMA expression on human MM cell lines, which is high in H929 cells and relatively low on L363 cells (Supplementary Fig. 1A). To further explore whether MCL-1 inhibition sensitizes MM cells to anti-BCMA CAR T cells, we performed a sequential treatment assay where patient-derived MM cells were exposed to MCL-1i for 48 h before co-culture with anti-BCMA CAR T cells. MCL-1i pre-treated primary MM cells were significantly more sensitive to anti-BCMA CAR T cells than their non-pre-treated counterparts (Fig. 1F and Supplementary Fig. 1B, C). These experiments combined illustrate that anti-BCMA CAR T cell-mediated MM cell killing can be enhanced by targeting of MCL-1 and suggest that combined treatment may be clinically advantageous.

Although MCL-1 is a bona fide MM target, it is also present in healthy cells and tissues, and should be inhibited in MM cells specifically to allow safe and effective treatment. To target MCL-1 exclusively in cancer cells and avoid systemic toxicity we explored the possibility of MCL-1-inhibitor delivery via CAR T cells. First, we tested whether exogenous delivery of NOXA induces apoptosis in cancer cells that depend on MCL-1 expression for survival. MM cells were treated with synthetic NOXA together with sub-lytic concentrations of pore-forming protein streptolysin O (SLO) to facilitate NOXA delivery in target cells. We could visualize entry of fluorescently labeled synthetic NOXA (NOXA-TAMRA) into the cytosol of L363 MM or OCI-Ly10 DLBCL cells by confocal microscopy (Fig. 2A and Supplementary Fig. 2A) and revealed binding to intracellular MCL-1 by immunoprecipitation (Fig. 2B). The introduced NOXA promoted MM cell apoptosis in a dose-dependent manner, which shows that delivery of NOXA specifically into MCL-1-dependent tumor cells is sufficient to induce tumor cell killing (Fig. 2c–e and Supplementary Fig. 2b, c).

Next, we developed a strategy to load proteins of choice in cytotoxic granules of CAR T cells that can be released into target cells upon contact (Fig. 3A). The ultimate aim with this strategy is to boost CAR T cell cytotoxicity and kill additional cancer cells that would resist killing by standard CAR T cell mechanisms, including release of cytotoxic granules containing perforin and granzymes, and ligation of death receptors on cancer cells. To achieve this, we cloned cargo proteins, including the red fluorescent protein mScarlet, behind the sequence encoding granzyme B in a lentiviral vector (Fig. 3B). Using confocal microscopy we confirmed that these cargo proteins localize to LAMP-1-positive cytotoxic granules in transduced primary human T cells (Fig. 3C). Next, we transduced anti-BCMA CAR T cells with the construct shown in Fig. 3B and co-cultured these with MM cells. In time, accumulation of fluorescent mScarlet could be detected in the targeted MM cells (Fig. 3D, E). EGFP, which was placed behind a T2A sequence and not directly located behind the granzyme B sequence, was not localized to cytotoxic granules in transduced anti-BCMA CAR T cells and was therefore not delivered to MM cells after co-culture (Fig. 3C, D, F). Replacing mScarlet by the more stable fluorescent protein mNeonGreen allowed visualizing cargo transfer in timelapse confocal imaging (Supplementary Fig. 3a). Co-culture of anti-BCMA CAR T cells transduced with the Granzyme B-mNeonGreen construct

https://doi.org/10.1038/s41467-025-59818-8

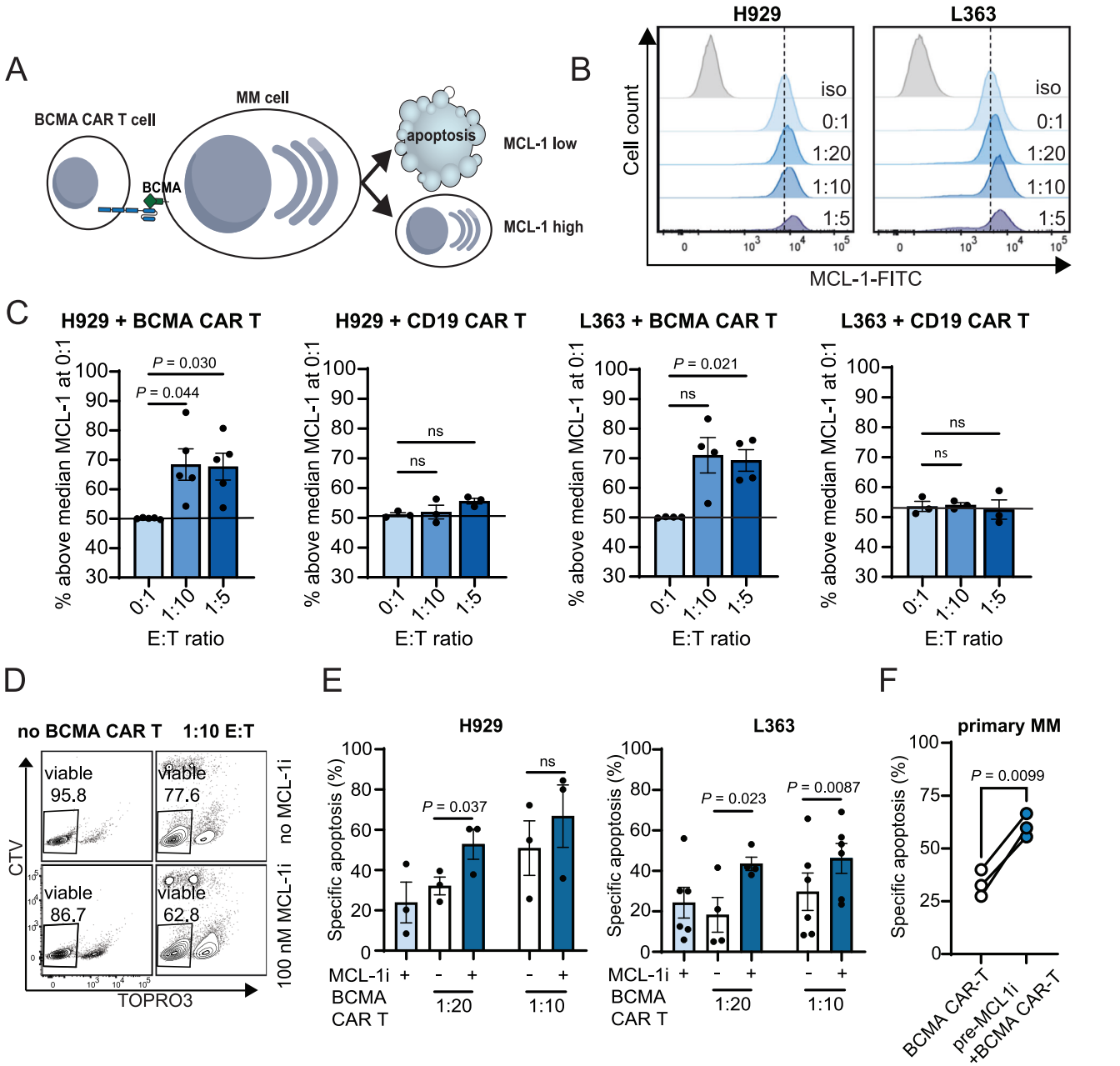


**Fig. 1 | MCL-1 expression limits MM cell killing by anti-BCMA CAR T cells.** **A** Graphical representation of experimental findings. **B** Representative histograms showing MCL-1 protein expression measured by intracellular flow cytometry in alive H929 or L363 MM cells after 24 h co-culture with anti-BCMA CAR T cells using the indicated effector to target cell ratio's (E:T). The dotted line indicates the median fluorescence intensity of MCL-1 in untreated (0:1) L363 or H929 cells. The gray histograms shows isotype control staining (iso). **C** H929 and L363 cells were co-cultured for 24 h with either anti-BCMA CAR T (H929, $n = 5$; L363, $n = 4$) or CD19 CAR T ($n = 3$) cells at the E:T ratios specified. Graphs show the percentage of viable H929 or L363 with MCL-1 expression above the median expression in untreated cells. Dots represent separate experiments with SEM. Statistical testing was performed using one-way ANOVA, followed by multiple comparison testing. **D** Representative gating strategy of L363 MM cells co-cultured with CellTrace Violet (CTV)-labeled anti-BCMA CAR T cells and stained with nucleic acid dye TO-PRO-3, and measured by flow cytometry after 24 h of culture. Co-cultures were simultaneously incubated with 100 nM MCL-1 inhibitor S63845 (lower panels) or without (upper panels). Indicated percentages of viable cells are calculated within CTV-negative MM cells. **E** Quantified specific apoptosis of H929 or L363 cells as detailed for (**C**) and by using the gating strategy shown in (**D**). Percentages were calculated based on absolute cell numbers using counting beads. Specific apoptosis was determined by measuring the altered percentage of TO-PRO-3$^-$ (live) cells compared with untreated cells and was defined as follows: ([% cell death in treated cells–% cell death in control]/% viable cells control) × 100. For H929 a concentration of 10 nM MCL-1i and for L363 a concentration of 100 nM MCL-1i was used. Dots show averages of separate experiments with H929 ($n = 3$) or L363 ($n = 6$) with SEM. Statistical testing was performed using one-way ANOVA, followed by multiple comparison testing. **F** Specific apoptosis (calculated as in (**E**)) induced by anti-BCMA CAR T cells in primary MM cells pre-treated with MCL-1i (blue circles) or without pre-treatment (white circles). Bone marrow mononuclear cells (BMNCs) were cultured for 48 h in the presence or absence of MCL-1i (S63845, 100 nM). After pre-treatment, the number of viable MM cells (CD38 + CD138+) on each condition was quantified by FACS following the gating strategy shown in Supplementary Fig. 1c. MCL-1i was washed away and BMNCs cells were subsequently co-cultured with anti-BCMA CAR T cells for 24 h at a 1:5 E:T ratio, calculated based on the number of alive MM cells present on each condition. Data are from 3 independent experiments. Each circle represents a patient sample. Statistical analysis was performed using a two-tailed paired *t* test. Source data are provided as a Source Data file.

https://doi.org/10.1038/s41467-025-59818-8

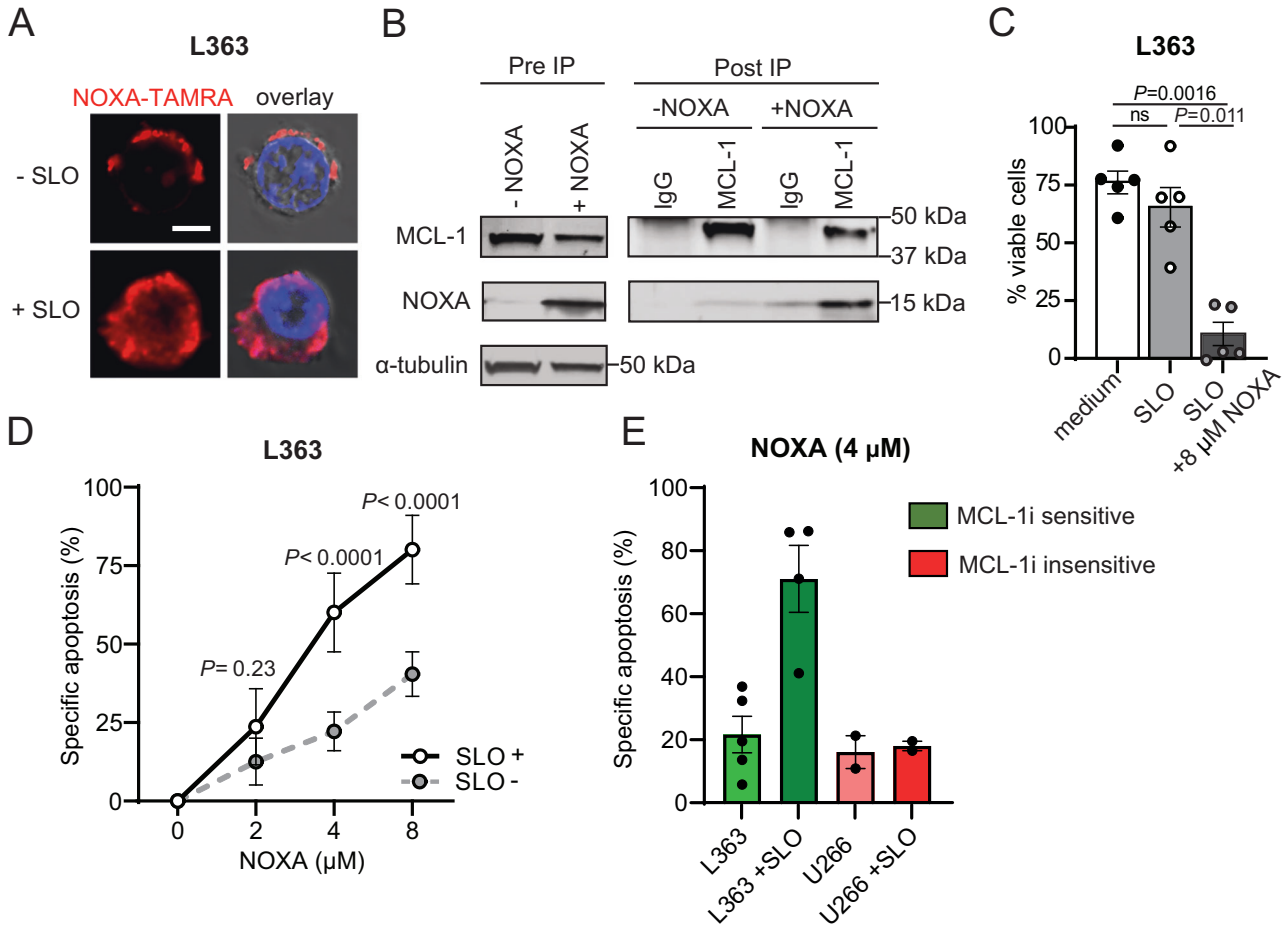


**Fig. 2 | Exogenous NOXA induces apoptosis in L363 cells. A**) Representative confocal image (630 × oil magnification) showing L363 MM cells incubated with 10 μM synthetic NOXA-TAMRA with or without 15 ng/ml streptolysin O (SLO). Scale bar, 5 μM. **B** SDS-PAGE electrophoresis of NP40 lysates from L363 MM cells treated with 15 ng/ml SLO, with or without 10 μM synthetic NOXA, stained for NOXA, MCL-1 and α-tubulin as control. Left panel shows the untreated lysates before immunoprecipitation (pre IP) and the right panel shows the cell lysates after immunoprecipitation with MCL-1 or control (IgG) antibodies (post- IP). **C** Percentage of viable ($DiOC6(3)^+TO\text{-}PRO\text{-}3^-$) L363 MM cells treated with 15 ng/ml SLO, with or without 8 μM synthetic NOXA and analyzed by flow cytometry following the gating strategy shown in Fig. 1d. Shown are averages of 5 biological replicates with SEM. Statistical analysis was performed using a one-way ANOVA with Geisser-Greenhouse correction. **D** Apoptosis induced by synthetic NOXA in L363 MM cells treated with 15 ng/ml SLO or without SLO, analyzed by flow cytometry with viability dyes TO-PRO-3 and DiOC6(3). Shown are averages of 5 biological replicates with SEM. Statistical analysis was performed using a two-way ANOVA followed by multiple comparison testing. **E** Specific apoptosis induced in L363 or U266 MM cells treated with 15 ng/ml SLO, with or without 4 μM synthetic NOXA and analyzed by flow cytometry. Dots represent separate experiments with SEM. Source data are provided as a Source Data file.

together with MM H929 cells showed re-localization of mNeonGreen to the synapse with MM cells, followed by delivery of a portion of the mNeonGreen cargo from the CAR T cells into the cytosol of MM cells (Supplementary Fig. 3b). Combined, these experiments reveal that using our strategy proteins of choice can be localized to cytotoxic granules in CAR T cells and delivered specifically into targeted cancer cells upon contact.

To test improved killing of MCL-1-dependent cancer cells by CAR T cells, we cloned the sequence encoding NOXA behind granzyme B, as we did for mScarlet (Fig. 4A). As control, we introduced 3 point mutations in the BCL-2 homology 3 (BH3) domain of NOXA, which is used for binding and inhibiting MCL-1 (Fig. 4A). These point mutations render NOXA inactive (iNOXA) and unable to bind MCL-1[21]. By using HA-tagged versions of NOXA and iNOXA we could visualize their intracellular localization in transduced T cells. As expected from our findings with fluorescent cargo molecules (Fig. 3C), we observed that NOXA and iNOXA localize to LAMP-1-positive cytotoxic granules in transduced primary T cells or in NK cell line YT-Indy (Fig. 4B and Supplementary Fig. 4a, b). Anti-BCMA CAR T cells transduced with constructs containing NOXA (NOXA-BCMA CAR T cells) increased apoptosis of MM cell lines H929 (Fig. 4C) and RPMI-8226 (Supplementary Fig. 5a), as well as primary MM cells (Fig. 4D), compared to control anti-BCMA CAR T cells transduced with iNOXA (iNOXA-BCMA CAR T cells). Our findings were not only restricted to anti-BCMA CAR T cells since YT-Indy NK cells transduced with constructs containing NOXA killed H929 MM cells (Supplementary Fig. 5b) and diffuse large B cell lymphoma (DLBCL) cell line OCI-Ly7 (Supplementary Fig. 5c) better than NK cells transduced with iNOXA. To confirm improved killing by NOXA-BCMA CAR T cells in vivo, we performed mouse xenograft experiments. Here, immunodeficient NOD SCID gamma (NSG) mice were intravenously injected with luciferase-transduced RPMI-8226 MM cells. Three weeks after tumor engraftment, when tumor cells could be visualized, NOXA-BCMA or iNOXA-BCMA CAR T cells were intravenously injected ($0.8 \times 10^6$ CAR T cells per mouse in a 1:1 CD4:CD8 T cell ratio) and tumor growth was monitored in time using bioluminescence imaging (BLI) (Fig. 5A). In this in vivo model, MM outgrowth was significantly delayed in mice receiving NOXA-BCMA CAR T cells as compared to mice receiving iNOXA-BCMA CAR T cells, similar to in vitro observations (Fig. 5B, C). This xenograft experiment was repeated with a fixed endpoint at day 14 to assess the presence and phenotype of cytotoxic NOXA-BCMA CAR T and iNOXA-BCMA CAR T cells in different organs. In line with the

https://doi.org/10.1038/s41467-025-59818-8

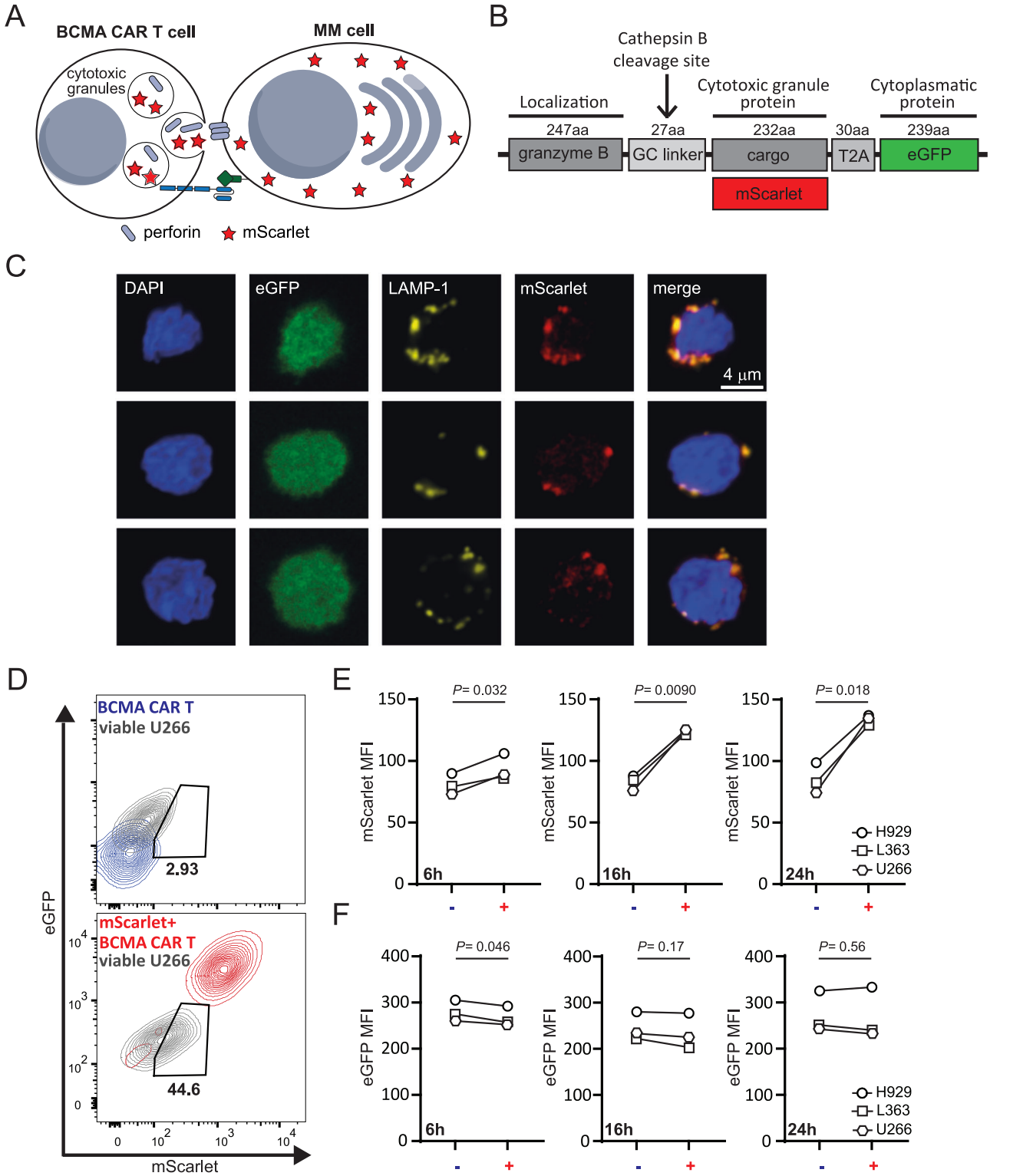


**Fig. 3 | anti-BCMA CAR T cells can be equipped with fluorescent cargo that is transferred to MM cells upon cell-cell interaction. A** Graphical representation of experimental findings. **B** Construct design with cargo proteins fused to granzyme B through a GC linker that contains a cathepsin B cleavage site. **C** Representative confocal images (×630 oil-magnification) of anti-BCMA CAR T cells transduced with the lentiviral construct shown in (**B**) and stained for late endosomal marker LAMP-1 and DAPI. **D** Representative image of eGFP and mScarlet fluorescence in viable U266 MM cells (gray) when co-cultured with WT (blue) or mScarlet$^+$ (red) anti-BCMA CAR T cells for 24 h in a 1:5 E:T cell ratio. Fluorescence signals of WT or mScarlet$^+$ anti-BCMA CAR T cells were used as overlay in these plots to indicate range of eGFP and mScarlet expression. **E**, **F** Mean fluorescence intensity (MFI) of mScarlet (**E**) or eGFP (**F**) in the total viable population of indicated target MM cell lines ($n = 3$) when co-cultured for 6, 16, or 24 h with WT (−) or mScarlet$^+$ (+) anti-BCMA CAR T cells in a 1:5 E:T cell ratio. The experiment was performed in the presence of 10 µM caspase inhibitor Q-VD-OPh to inhibit apoptosis of target cells. Statistical analysis was performed using a paired, two-tailed *t* test. Source data are provided as a Source Data file.

https://doi.org/10.1038/s41467-025-59818-8

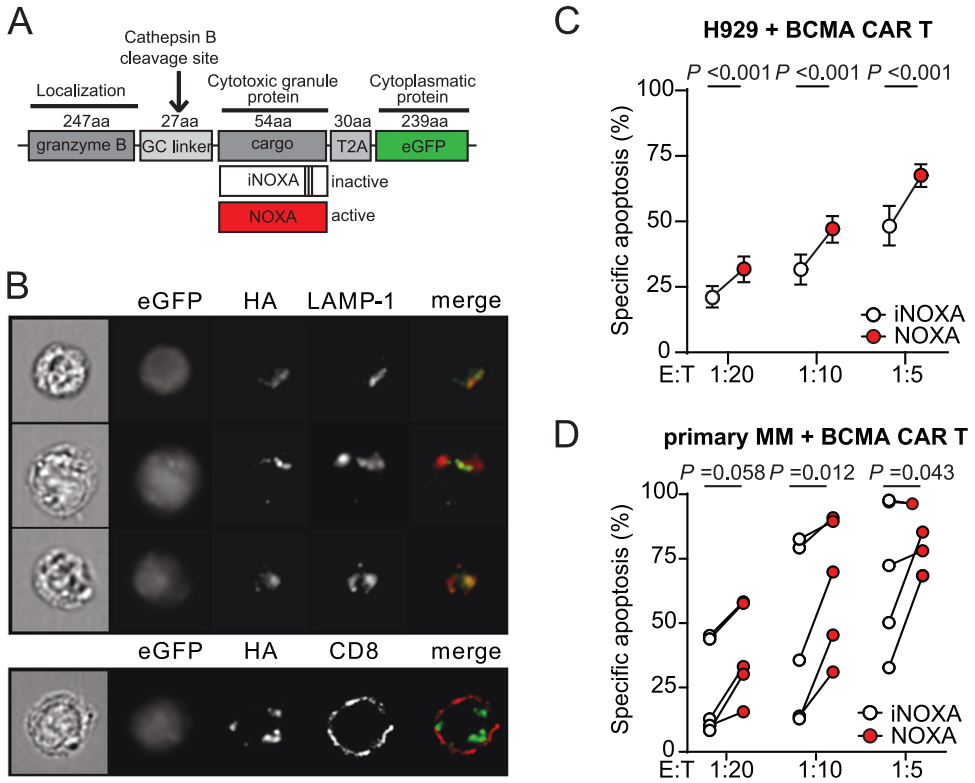


**Fig. 4 | Anti-BCMA CAR T cells armed with NOXA show improved killing of MM cells. A** Construct design with pro-apoptotic NOXA (active) or mutated (inactive) NOXA (iNOXA) as cargo proteins fused to granzyme B. **B** Representative image-based flow cytometry image captures by ImageStream at ×1060 magnification of CD8⁺ anti-BCMA CAR T transduced with the constructs depicted in (**A**) and stained with antibodies against HA and LAMP-1 or CD8. **C** Specific apoptosis induced in H929 cells after 24 h of co-culture with NOXA-BCMA CAR T cells or iNOXA-BCMA CAR T cells at indicated E:T cell ratios. Apoptosis was analyzed by flow cytometry following the gating strategy shown in Fig. 1D. Values are average of 7 independent experiments with SEM. Statistical testing was performed using a two-way ANOVA followed by a Sidak's multiple comparison test. **D** Specific apoptosis induced in primary CD38⁺CD138⁺ MM cells after 48 h of co-culture with NOXA-BCMA CAR T cells or iNOXA-BCMA CAR T cells at indicated E:T cell ratios. Apoptosis was analyzed by flow cytometry following the gating strategy shown in Supplementary Fig. 1c. Each dot represents a different MM patient sample ($n = 5$). Statistical testing was performed using a two-way ANOVA followed by a Sidak's multiple comparison test. Source data are provided as a Source Data file.

previous assay, tumor load was reduced in mice treated with NOXA-BCMA CAR T cells (Supplementary Fig. 6a). The proportion of CD8⁺ CAR T cells in the spleen was comparable between NOXA- and iNOXA-BCMA CAR T cell-treated mice (Supplementary Fig. 6b, c). Expression of both PD-1, an exhaustion-related marker, and Fas ligand (FASL/CD95L), the main death receptor ligand, was comparable between NOXA-BCMA and iNOXA-BCMA CAR T cells (Supplementary Fig. 6b). Next to the described model with established RPMI-8226 tumors, we also performed xenograft experiments where NSG mice were intravenously injected with luciferase-transduced NCI-H929 MM cells. Here, NOXA-BCMA or iNOXA-BCMA CAR T cells were intravenously injected ($1.0 \times 10^6$ CAR T cells per mouse in a 1:1 CD4:CD8 T cell ratio) one week after tumor engraftment (Fig. 5E). In line with the previous xenograft model we observed a significant delay in MM outgrowth in mice receiving NOXA-BCMA CAR T cells as compared to mice receiving iNOXA-BCMA CAR T cells, as measured by BLI imaging (Fig. 5F, G).

To examine potential toxicity to healthy cells in the local microenvironment in more detail, we tested NOXA-BCMA CAR T cell-mediated toxicity to non-targeted BM cells from MM patients in co-culture experiments. Although a clear reduction in MM cells could be measured comparing co-cultures with NOXA-BCMA versus iNOXA-BCMA CAR T cells, no differences in the viability of other healthy BM cells were observed (Fig. 6A, B). This indicates there is no apparent toxicity to non-targeted BM cells. Since it was described that MCL-1 inhibition can cause cardiac failure in vivo and apoptosis induction of human iPSC-derived cardiomyocytes in vitro, we examined whether NOXA-BCMA CAR T cells displayed toxicity to cardiomyocytes[22,23]. We generated human iPSC-derived cardiomyocytes (CMs) and confirmed toxicity of MCL-1i as measured by the percentage of metabolically active CMs and presence of beating CMs by microscopy (Fig. 6C, D and Supplementary Movies 1–6)[24]. Likewise, we confirmed that exogenous NOXA, which is actively taken up from the supernatant by CMs (Supplementary Fig. 7a), is toxic to CMs at dosages of 4 or 8 µM. Next, we generated anti-BCMA CAR T cells with 3 NOXA repeats following the granzyme B sequence to test possible toxicity due to NOXA secretion by the CAR T cells or due to possible leakage of NOXA from dying anti-BCMA CAR T or targeted MM cells (Supplementary Fig. 7b, c). We did not observe any toxicity to CMs after 24 h co-culture of CMs with NOXA$^{3X}$ anti-BCMA CAR T cells and H929 MM cells, while 88–91% of H929 cells were killed (Fig. 6C, D and Supplementary Movies 1–6). In fact, a small increase in metabolic activity was observed in the triple co-culture which could be explained by the remaining H929 that are metabolically active. Combined, these data show that the amount of NOXA, if any, that is released into the environment is too low to induce toxicity to surrounding cells.

While NOXA was predominantly localized to granules in transduced T cells (Figs. 3C, B) or NK cells (Supplementary Fig. 4b), it is possible that a portion of the introduced NOXA mis-localizes to -or leaks from- cytotoxic granules, resulting in toxicity to the T cells themselves. Therefore, we examined viability of transduced NOXA-BCMA versus iNOXA-BCMA CAR T cells during a 2-month in vitro culture period but did not observe differences in viability, while

https://doi.org/10.1038/s41467-025-59818-8

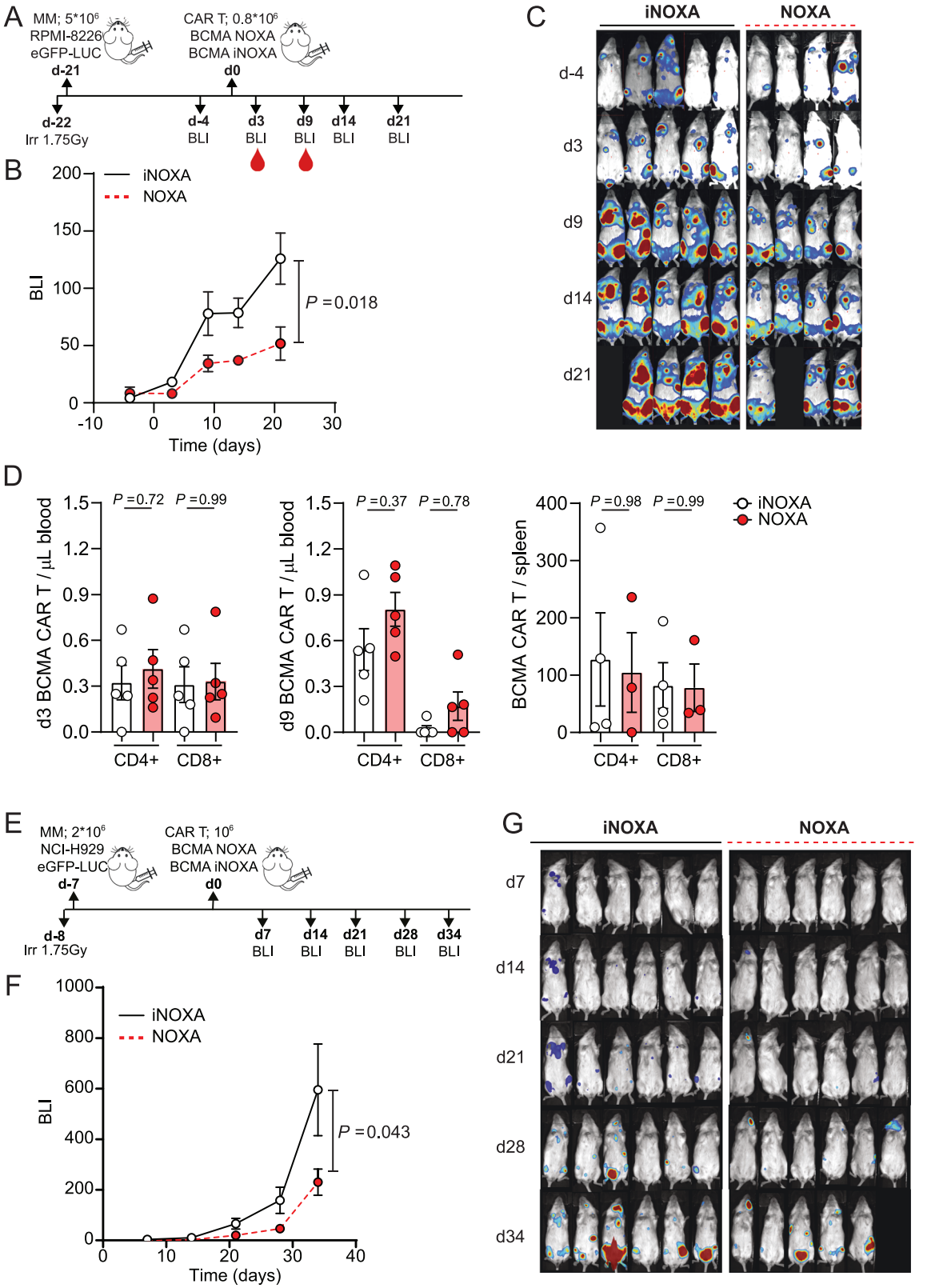


CD4:CD8 ratios and transcript expression remain comparable (Supplementary Fig. 8). Moreover, we examined presence of transduced NOXA-BCMA versus iNOXA-BCMA CAR T cells in blood and in the spleen of mice in a xenograft model that was previously outlined in Fig. 5A–C and Supplementary Fig. 6. This analysis reveals that addition of functional NOXA does not hamper in vivo persistence of anti-BCMA CAR T cells (Fig. 5d and Supplementary Fig. 8).

## Discussion

Collectively, our data show that, by making use of the natural properties of granzyme B, we can direct pro-apoptotic proteins, such as NOXA, specifically into MM cells upon interaction with anti-BCMA CAR T cells and subsequently promote apoptosis. As a consequence there is improved killing of cancer cells and diminished primary resistance. Importantly, resistance of tumor cells to undergo apoptosis after CAR

**Fig. 5 | NOXA-BCMA CAR T cells show improved killing of MM cells in vivo.** **A** Experimental setup of xenograft mouse experiment where NSG mice are i.v. injected with RPMI8226-eGFP-Luc2 MM cells, followed by i.v. injection of indicated anti-BCMA CAR T cells ($0.8 \times 10^6$, with a 1:1 CD4:CD8 ratio) 21 days later. Blood samples were taken at day 3 and 9 post-CAR T injection. **B** Average bioluminescence intensity (BLI) (flux p/s) of mice treated with NOXA-BCMA ($n = 4$) or iNOXA-BCMA CAR T ($n = 5$) over time with SEM. Statistical testing was performed using a mixed-effect model followed by Sidak's multiple comparison test. **C** Corresponding BLI images of mice shown in (**B**). **D** Number of $CD4^+$ and $CD8^+$ iNOXA-BCMA or NOXA-BCMA CAR T cells in blood at 3 (left panel) or 9 (center panel) days, or in the spleen (days 25–27, right panel), after i.v. injection in mice as outlined in (**A**). Cells were analyzed by flow cytometry following the gating strategy shown in Supplementary Fig. 6b. Statistical testing was performed using one-way ANOVA, followed by multiple comparison testing. **E** Experimental setup of xenograft mouse experiment where NSG mice are i.v. injected with NCI-H929-eGFP-Luc2 MM cells, followed by i.v. injection of indicated anti-BCMA CAR T cells ($1.0 \times 10^6$, with a 1:1 CD4:CD8 ratio) 7 days later. **F** Average bioluminescence intensity (BLI) (flux p/s) of mice treated with NOXA-BCMA ($n = 6$) or iNOXA-BCMA CAR T ($n = 6$) over time with SEM. Statistical testing was performed using a mixed-effect model followed by Sidak's multiple comparison test. **G** Corresponding BLI images of mice shown in (**F**). Images in (**A**) and (**E**) indicating experimental setups were adapted from Sun et al.[41]. Source data are provided as a Source Data file.

T cell treatment is an immune escape mechanism that is not only confined to MM[2,3]. Therefore, tumor cell killing by CAR T cells in general should be improved to create an optimal CAR T cell therapy for more indications. Different strategies have been published that describe arming of CAR T cells and are referred to as armored CAR T cells or TRUCKs (T cells redirected for universal cytokine-mediated killing). Initially, T cells were created that constitutively express IL-12 or IL-18 to influence the tumor microenvironment and potentiate the antitumor response[25–27], but after safety concerns TRUCKs were created with inducible IL-12 expression[28]. Since, a plethora of TRUCKs have been developed able to express a range of different cytokines to aid the anti-tumor response[26,29]. With these approaches secretion is not directed specifically towards cancer cells. In contrast, our optimized killing strategy for CAR T cells delivers a pro-apoptotic molecule specifically into cancer cells that interacted with a CAR T cell. Due to the directed secretion that is limited to the immune synapse, toxicity of pro-apoptotic cargo to neighboring cells is expected to be minimal. The possibility to equip NK cells with protein cargo that can be transferred to target cells via the granzyme-perforin pathway has previously been shown using fluorescent molecules and further validates our strategy[30].

The effective combination treatment with anti-BCMA CAR T cells and MCL-1 inhibitors shown in Fig. 1d–f may indicate therapeutic potential. However, we and others have shown that MCL-1 expression sustains survival of many healthy cells and tissues and co-treatment with a systemic MCL-1 inhibitor would generate undesired side-effects, precluding its use as a safe anti-cancer drug[31–35]. For example, it was shown that genetic deletion of *Mcl1* in mice causes lethal cardiac failure and that MCL-1 inhibition promotes apoptosis of human iPSC-derived cardiomyocytes[22,23]. Regardless of these findings, multiple pharmaceutical companies generated MCL-1-specific inhibitors for treatment of MM, acute myeloid leukemia (AML) and B cell lymphoma that were tested in phase I clinical trials. Currently, most of these clinical trials have been put on FDA-instructed or voluntary hold due to dose-related cardiac toxicity[36].

By arming CAR T cells with NOXA we have demonstrated the possibility to improve killing of cancer cells dependent on MCL-1 expression for survival. However, this approach might not be sufficient for other tumor types that are MCL-1-independent. Pro-apoptotic proteins, besides NOXA, specifically inhibiting other pro-survival BCL-2 family proteins can be used in this setting. Alternatively, additional proteins that promote apoptotic or immunogenic cell death can be used to arm engineered T or NK cells and increase therapy options in a tailor-made fashion. Next to promoting cell death directly, other processes can be manipulated in targeted cancer cells by activating kinases or pathways, as shown previously using a synthetic enzyme-armed killer (SEAKER) CAR T cell strategy[37]. To examine CAR T cell behavior in more detail our strategy can also be employed using fluorescent molecules as cargo. This approach allows quantification of cargo transfer in relation to CAR T cell activation status, cellular interaction time and serial killing efficacy, and may provide clues for further optimization of CAR T cell technology.

# Methods

## Cell culture and chemicals

A detailed overview of all antibodies, reagents and cell lines used in this study is provided in Supplementary Table 1. Cells were cultured in Dulbecco´s Modified Eagle Medium (DMEM, Life Technologies) (Phoenix-Ampho, HEK293T), Iscove´s Modified Dulbecco´s Medium (IMDM, life Technologies) (OCI-Ly7), or RPMI 1640 GlutaMAX HEPES culture medium (Life Technologies) (L-363, U-266, MM1.s, RPMI-8226-GFP-Luc2, YT-Indy and pMM), supplemented with 10–20% fetal bovine serum (FBS, Sigma) and 100 μg/mL penicillin-streptomycin (p/s, Gibco/Life Technologies). For NCI-H929 cells 50 μM β-mercaptoethanol (Life Technologies) was added to the culture medium. All primary MM samples were obtained after written informed consent, and protocols were approved by the local ethics committee of the University Medical Center Utrecht. Clinical characteristics of the patient samples included are listed in Supplementary Table 2. For primary MM cell culture, the medium was supplemented with 100 ng/mL human recombinant IL-6 (PeproTech) and 100 ng/mL human recombinant APRIL/TNFSF-13 (R&D systems). For sequential treatment assays, frozen bone marrow mononuclear cells (BMNCs) obtained from BM aspirates of MM patients were thawed and the proportion and number of alive plasma cells ($CD38^+CD138^+$) was determined by FACS. BMNCs were then split into two wells (untreated or treated with 100 nM of S63845 (Servier)) and cultured for 48 h in medium supplemented with IL-6 and APRIL. After this time, the proportion and number of alive $CD38^+CD138^+$ cells per condition was measured again by FACS. Anti-BCMA CAR T cells were labeled with CellTrace Violet (Life Technologies) following the manufacturer's instructions. Co-cultures were established with at least 25,000 alive MM cells per condition, and anti-BCMA CAR T cells were added at the E:T ratios specified. After 24 h co-culture, the proportion of viable (TO-PRO-3$^-$, Invitrogen) MM cells was determined by FACS.

## Apoptosis staining and flow cytometry

Assessment of cell viability was performed by staining with 20 nM TO-PRO-3 (Invitrogen) or with Fixable Viability Dye (FVD) eFluor506 or eFluor780 (eBioscience), followed by flow cytometric analysis (BD FACSCanto II or BD LSRFortessa, BD Biosciences). To determine the absolute amount of cells Flow count Fluorospheres were used (Beckman Coulter). In co-culture experiments, target cells were identified by flow cytometric surface staining with CD38-PE (Invitrogen) and CD138-PERCP-Cy5.5 (Biolegend) (DL-101) (primary MM cells), or by staining with CellTrace Violet (Life Technologies) (MM cell lines) prior to adding effector cells. Anti-BCMA CAR T cells were characterized by staining with CD4-Pacific Blue (Biolegend) (RPA-T4), CD8-PE/Cy7 (BD) (SK1), and biotinylated human BCMA (Sino Biological) with streptavidin-PE (BD Pharmingen). For intracellular staining, cells were fixed and permeabilized using BD Cytofix/Cytoperm (BD Biosciences), and stained with rabbit anti-MCL-1 (Abcam) (Y37), rabbit anti-HA-TAG (CST) (C29F4), donkey anti-rabbit-IgG-Alexa Fluor 488 (Biolegend). Exhaustion and death receptor ligand expression on anti-BCMA CAR T cells from murine spleens was analyzed using anti-PD-1 (Biolegend)

https://doi.org/10.1038/s41467-025-59818-8

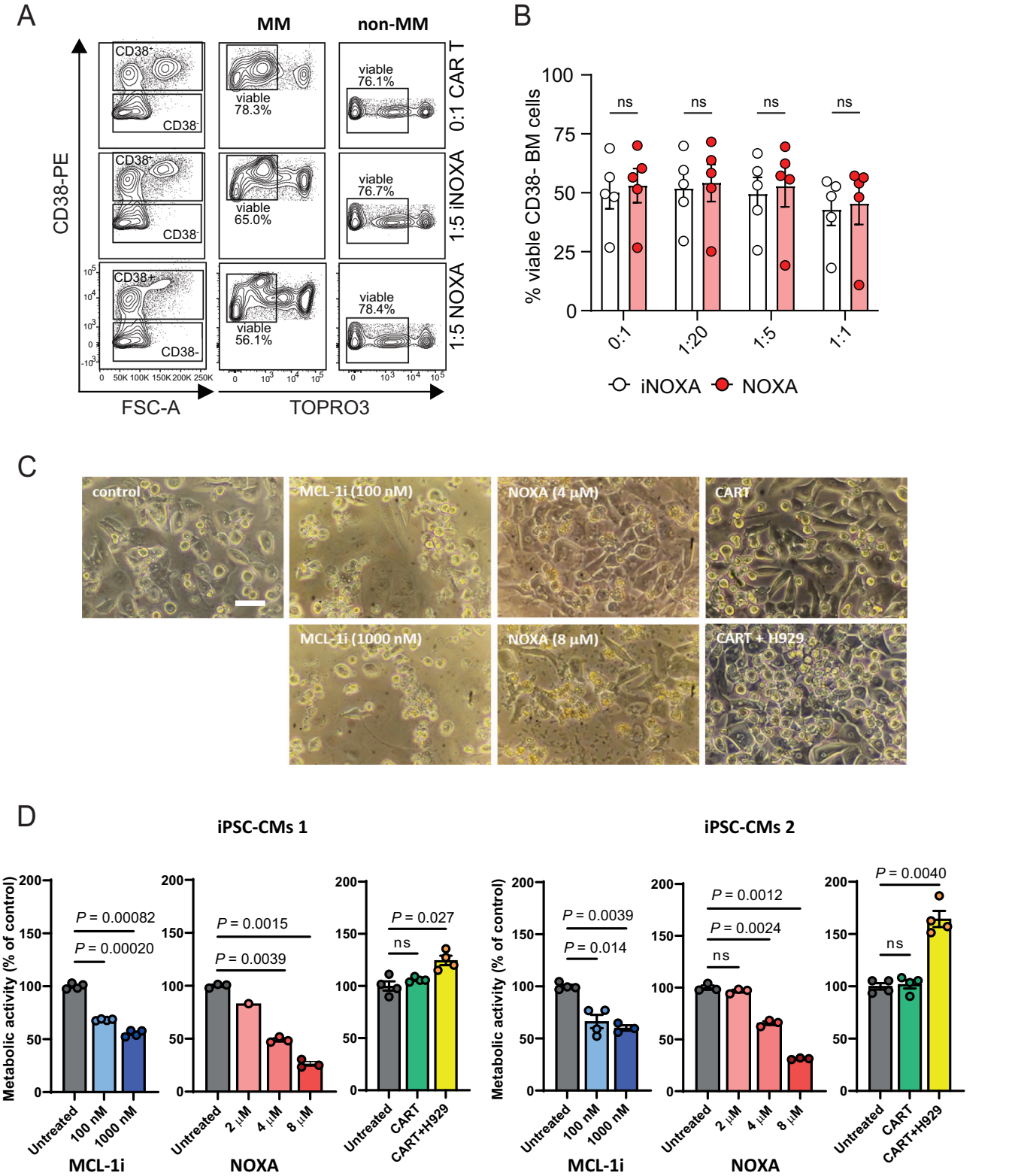


**Fig. 6 | NOXA cargo does not impair viability of transduced anti-BCMA CAR T cells and does not show off-target toxicity.** Representative density plots showing cell viability (TO-PRO-3 staining) of primary bone marrow stromal cells ($CD38^-$) or MM ($CD38^+$) cells after 48 h of co-culture with iNOXA-BCMA or NOXA-BCMA CAR T cells in a 1:5 E:T cell ratio or without anti-BCMA CAR T cells (0:1 E:T). **B** Quantification of data shown in (**A**) with each dot representing a different MM patient sample ($n = 5$) co-cultured with iNOXA-BCMA or NOXA-BCMA CAR T cells at indicated E:T ratios for 48 h. Dots represent separate experiments with SEM. Statistical testing was performed using a two-way ANOVA followed by Sidak's multiple comparison test. **C** Representative microscope images (bright field) of hiPSC-CMs ($1 \times 10^5$ per well) are shown that are untreated (control), treated for 24 h with indicated dosages of MCL-1i (S63845) or synthetic NOXA, or after a 24 h co-culture with $NOXA^{3X}$ BCMA CAR T cells ($0.5 \times 10^5$ per well) alone or together with H929 MM cells ($0.5 \times 10^5$ per well). Scale bar, 200 μM. Matching video files showing the beating rate of indicated conditions are uploaded as Supplementary Movies 1–6. **D** AlamarBlue assays representing the metabolic activity per well in conditions outlined in (**C**). Two different hiPSC donors were used. Each dot represents a separate experiment ($n = 1$–4) with SEM. Statistical testing was performed using one-way ANOVA, followed by multiple comparison testing. Source data are provided as a Source Data file.

(EH12.2H7) and anti-FasL (Biolegend) (NOK.1), respectively. Flow cytometry data analysis was performed using FlowJo.

### Generation of anti-BCMA and anti-CD19 CAR T cells

An overview of all amino acid sequences for the constructs used in this study is provided in Supplementary Table 3. The anti-BCMA CAR construct (pBu-BCMA-CAR) was generated by cloning single-chain variable fragments from anti-BCMA antibody into a pBullet vector containing a D8α-41BB-CD3-ζ signaling cassette. Phoenix-Ampho packaging cells were transfected with gag-pol (pHit60), env (P-COLT-GALV) and pBu-BCMA-CAR or pBu-CD19-CAR, using Fugene HD transfection reagent (Promega). Human healthy donor peripheral blood mononuclear cells (PBMC) were isolated from buffy coats (Sanquin, Amsterdam, the Netherlands) using Ficoll-Paque according to the manufacturer´s protocol. PBMC were cultured in RPMI with 2.5% pooled AB+ human serum (IPLA-CSER, Innovative Research), 50 µM β-mercaptoethanol (Life Technologies) and 1% p/s. PBMC were pre-activated with 30 ng/ml anti-CD3 (OKT3, Biotec) and 50 IU/mL IL-2 (Sigma) and subsequently transduced two times with viral supernatant in the presence of 6 ug/ml polybrene (Sigma) and 50 U/ml IL-2. Transduced T cells were expanded using 50 U/ml IL-2 and anti CD3/CD28 dynabeads (Gibco), and anti-BCMA- or anti-CD19-CAR-expressing cells were selected by treatment with 80 µg/mL geneticin. T cells were further expanded using a rapid expansion protocol (REP)[38]. In short; T cells were co-cultured with irradiated feeder cells (total of $12.5 \times 10^6$ PBMCs of 3 different donors and $2.5 \times 10^6$ LCL cells), OKT-3 (30 ng/mL), IL-2 (50 U/mL), IL-15 (5 ng/mL) and PHA-L (1 µg/mL) in RPMI-1640 (Gibco) supplemented with 1% p/s, 2.5% pooled AB+ serum and 50 µM β-mercaptoethanol for 3 days. On day 4 medium was replaced with above made medium and added IL-2 (50 U/mL). This medium change was also done on day 7 and 11. For transduction with our granzyme B – cargo – T2A - eGFP constructs, gBlocks (IDT) were cloned into lentiviral vector pCCL. For co-culture experiments with CMs, we generated an "all-in-one" integrated lentiviral vector combining the granzyme B –cargo followed by a T2A self-cleaving peptide, and the anti-BCMA CAR. Here, we cloned as cargo three repeats of the NOXA encoding sequence, interspaced with cathepsin B cleavable linkers. Lentiviral particles were produced by transient transfection of the lentiviral vector and the packaging plasmids pRSV-Rev, pMDLg/pRRE, and pMD2-VSV-G to HEK293T cells using the CalPhos Mammalian Transfection Kit (Clontech Laboratories). Viral supernatants were filtered through 0.45 µm low-protein-binding filters (Sarstedt), concentrated by ultracentrifugation at 20,000 × *g* for 2 h, resuspended in StemMACS (Miltenyi Biotec), and stored at −80 °C. Previously transduced PBMC expressing an anti-BCMA CAR were transduced with the granzyme B-cargo-expressing lentiviral vector and eGFP-positive anti-BCMA CAR T cells were subsequently sorted (Sony MA900) and expanded on a rapid expansion protocol.

### Animal models

Female NOD.Cg-Prkdc$^{scid}$Il2rg$^{tm1Wjl}$/SzJ (NSG) mice (Charles River, strain code 614) age 8–12 weeks were ordered and temporarily housed in the Central Animal Facility of Utrecht University during the experiments. Animal care and handling were performed in accordance with the 'European Directive for the Protection of Vertebrate animals used for Experimental and Scientific Purpose, European Community Directive 86/609/CEE'. All experiments were approved by the Animal Welfare Body of the Utrecht University, The Netherlands. Mice were co-housed on a barrier section in individually ventilated cage (IVC) system to maintain sterile conditions and fed with sterile food and water. After irradiation, mice were given the antibiotic ciproxin in the sterile water throughout the duration of the experiment. Mice were randomized with equal distribution among the different groups, based on tumor size (measured with Bioluminescence Imaging (BLI) on day −1) for experiments described in Fig. 3D–F and Supplementary Fig. 6 or randomly distributed in Fig. 3G–I. Age and weight of mice were comparable between groups. Mice received sublethal total body irradiation (1,75 Gy) on day −22 followed by intravenous injection of $5 \times 10^6$ RPMI-8226-luciferase tumor cells on day −21, and received 1 intravenous injection of $0.8 \times 10^6$ NOXA-BCMA CAR T cells or iNOXA-BCMA CAR T cells on day 0. Alternatively, mice received sublethal total body irradiation (1.75 Gy) on day −8 followed by intravenous injection of $2 \times 10^6$ NCI-H929-luciferase tumor cells on day -7, and received 1 intravenous injection of $1.0 \times 10^6$ NOXA-BCMA CAR T cells or iNOXA-BCMA CAR T cells on day 0, comparable to recently described by Sun et al.[39]. Together with the CAR T cell injection, all mice received $0.6 \times 10^6$ IU of IL-2 (Proleukin; Clinigen) in 100 µl incomplete Freund's adjuvant (IFA). On day 3 and day 9, 50 µl of venous blood was drawn via cheek puncture to measure circulating anti-BCMA CAR T cell levels. Mice were monitored at least twice a week for any symptoms of disease (sign of paralysis, weakness, and reduced motility), weight loss, and clinical appearance scoring (scoring parameter included hunched appearance, activity, fur texture, and piloerection). The humane endpoint was reached when mice showed the aforementioned symptoms of disease or experienced a 20% weight loss from the initial weight (measured on day 1). During the experiment tumor growth was monitored weekly by BLI measurement after intraperitoneal (IP) Luciferin (Promega) injection. Mice were terminated via cervical dislocation when human endpoint was met or at the end of the experiment.

### Exogenous delivery of NOXA

In order to determine the effect of NOXA mediated killing, the pore forming Streptolysin O (S5265-25KU, Sigma) was used to facilitate entry of exogenous NOXA into target cells. SLO was activated with 10 mM DTT (Sigma-Aldrich) for 20 min at RT and subsequently diluted in serum-free RPMI. Target cells were incubated with SLO and synthetic NOXA or NOXA-TAMRA (provided as a gift by the Department Cell and Chemical Biology, Leiden University Medical Centre) for 30 min at 37 °C, after which FBS-containing medium was added to inactivate the SLO. After 24 h, apoptosis staining was performed to measure target cell viability using flow cytometry.

### Immunoblotting

For western blot analysis, cells were lysed in buffer containing 1% NP-40 and proteins were separated using SDS-PAGE (Mini-PROTEAN® TGX™ Precast Gels, Bio-Rad), transferred to low fluorescence PVDF membranes (Bio-Rad), blocked in phosphate-buffered saline (PBS, mediaroom UMCU) containing 2% non-fat dry milk, and stained using the following antibodies: mouse anti-α-tubulin (Cell signaling technology) (DM1A), mouse anti-NOXA (Abcam) (114C307.1), rabbit anti-MCL-1 (Novus-Biologicals) (Y37), goat anti-mouse-680RD, and goat anti-rabbit-800CW (LI-COR Biosciences). To enrich for MCL-1 binding protein immunoprecipitation was preformed using the Dynabeads Protein G IP Kit (Invitrogen) following the manufacturer's protocol. Infrared imaging was used for detection (Odyssey Sa; LI-COR Biosciences). Analysis and quantification were performed using LI-COR Image Studio and ImageJ 1.47V software.

### Microscopy

To visualize mScarlet, mNeongreen or NOXA, CAR T cells were placed on coverslips containing 0.1% poly-l-lysine (Sigma-Aldrich). Consequently, cells were fixed using 4% formaldehyde (VWR). For intracellular staining cells were blocked for 1 h using a blocking buffer consisting of 2% BSA (Sigma-Aldrich) and 0.1% saponin (Fisher Scientific) in PBS, followed by 1-h incubations with anti-LAMP-1 (BD or CST) (H4A3, BD Biosciences or D2D11, CST) or anti-HA tag (CST) (C29F4), in blocking buffer. After washing, the coverslips were mounted using ProLong Gold with DAPI (Invitrogen). Cells were imaged using a ×63 oil

lens (×630 total magnification) on a confocal microscope (Zeiss LSM710 (fixed) or Stellaris 5, Leica Microsystems (live imaging)). ImageJ was used to analyze the images.

### Cardiomyocyte experiments

Two hiPSCs lines, deposited in the European Bank for iPSCs (EBiSC, https://ebisc.org/) and registered in the online registry for human PSC lines hPSCreg (https://hpscreg.eu/), were used: UKKi037-C (NP0144-41; CM cell line 1) (male) and UKKi036-C (NP0143-18; CM cell line 2) (female)[40]. HiPSCs were differentiated into hiPSC-CMs using a GiWi differentiation protocol[24]. In short, at day 0, with hiPSCs at 90% confluency, medium was changed to heparin medium with 4 µM CHIR99021 (Selleck Chemicals). After 48 h, medium was refreshed with heparin medium with 2 µM Wnt-C59 (Tocris Bioscience). At day 4 and 6, medium was changed with heparin medium. From day 7 onwards, medium was replaced with insulin medium until purification around day 10. Around day 10, the hiPSC-CMs were beating, and medium was changed with purification medium every other day until day 15. Cellular metabolic activity of hiPSC-CMs was evaluated with the alamarBlue cell viability assay (Invitrogen, DAL1025) following the manufacturer's instructions. In short, 10% alamarBlue solution in construct medium was added to the constructs. After 4 h, the reacted solution was transferred to a 96-well plate and fluorescence was recorded using a fluorescence excitation wavelength of 560 nm and an emission wavelength of 590 nm. Absorbance was monitored at 570 nm and presented in arbitrary fluorescent units. To measure beating rate of hiPSC-CMs, 22 videos were taken using a GoPro Black Hero 7 camera connected to a bright field microscope (Olympus CKX41) via a c-mount system (Olympus U-TV1X-2). During video acquisition, cTE constructs were kept at 37 °C using a warm base plate.

### Statistical analysis

Statistical analysis was performed using GraphPad Prism version 8.3. Unpaired groups were compared with a Student's *t* test. For comparison of more than two groups, one-way or two-way ANOVA tests were used. Specific statistical test per experiment are indicated in the respective Figure legends. Error bars in figures are shown as standard error of the mean (SEM).

### Reporting summary

Further information on research design is available in the Nature Portfolio Reporting Summary linked to this article.

## Data availability

All data are included in the Supplementary Information or available from the authors, as are unique reagents used in this Article. The raw numbers for charts and graphs are available in the Source Data file whenever possible Source data are provided with this paper.

## References


1. Majzner, R. G. & Mackall, C. L. Clinical lessons learned from the first leg of the CAR T cell journey. *Nat. Med.* **25**, 1341–1355 (2019).
2. Melenhorst, J. J. et al. Decade-long leukaemia remissions with persistence of CD4(+) CAR T cells. *Nature* **602**, 503–509 (2022).
3. Sakemura, R. et al. Targeting cancer-associated fibroblasts in the bone marrow prevents resistance to CART-cell therapy in multiple myeloma. *Blood* **139**, 3708–3721 (2022).
4. Larson, R. C. & Maus, M. V. Recent advances and discoveries in the mechanisms and functions of CAR T cells. *Nat. Rev. Cancer* **21**, 145–161 (2021).
5. Newick, K., O'Brien, S., Moon, E. & Albelda, S. M. CAR T cell therapy for solid tumors. *Annu Rev. Med* **68**, 139–152 (2017).
6. Lee, Y. G. et al. Modulation of BCL-2 in Both T Cells and Tumor Cells to Enhance Chimeric Antigen Receptor T-cell Immunotherapy against Cancer. *Cancer Discov.* **12**, 2372–2391 (2022).
7. Yan, X. et al. Identification of NOXA as a pivotal regulator of resistance to CAR T-cell therapy in B-cell malignancies. *Signal Transduct. Target Ther.* **7**, 98 (2022).
8. Dufva, O. et al. Integrated drug profiling and CRISPR screening identify essential pathways for CAR T-cell cytotoxicity. *Blood* **135**, 597–609 (2020).
9. Singh, N. et al. Impaired death receptor signaling in leukemia causes antigen-independent resistance by inducing CAR T-cell dysfunction. *Cancer Discov.* **10**, 552–567 (2020).
10. Kimman, T. et al. Serpin B9 controls tumor cell killing by CAR T cells. *J. Immunother. Cancer* **11** (2023).
11. van Nieuwenhuijzen, N. et al. From MGUS to multiple myeloma, a paradigm for clonal evolution of premalignant cells. *Cancer Res.* **78**, 2449–2456 (2018).
12. Zheng, H. et al. BCMA-targeted therapies for multiple myeloma: latest updates from 2024 ASH annual meeting. *J. Hematol. Oncol.* **18**, 23 (2025).
13. Susanibar Adaniya, S. et al. CAR T cell therapy for multiple myeloma: what have we learned?. *Leukemia* **36** (2022).
14. Tiedemann, R. E. et al. Identification of molecular vulnerabilities in human multiple myeloma cells by RNA interference lethality screening of the druggable genome. *Cancer Res.* **72**, 757–768 (2012).
15. Slomp, A. & Peperzak, V. Role and regulation of pro-survival BCL-2 proteins in multiple myeloma. *Front Oncol.* **8**, 533 (2018).
16. Wuillème-Toumi, S. et al. Mcl-1 is overexpressed in multiple myeloma and associated with relapse and shorter survival. *Leukemia* **19**, 1248–1252 (2005).
17. Gomez-Bougie, P. et al. Noxa up-regulation and Mcl-1 cleavage are associated to apoptosis induction by bortezomib in multiple myeloma. *Cancer Res.* **67**, 5418–5424 (2007).
18. Guikema, J. E., Amiot, M. & Eldering, E. Exploiting the pro-apoptotic function of NOXA as a therapeutic modality in cancer. *Expert Opin. Ther. Targets* **21**, 767–779 (2017).
19. Kotschy, A. et al. The MCL1 inhibitor S63845 is tolerable and effective in diverse cancer models. *Nature* **538**, 477–482 (2016).
20. Slomp, A. et al. Multiple myeloma with 1q21 amplification is highly sensitive to MCL-1 targeting. *Blood Adv.* **3**, 4202–4214 (2019).
21. Czabotar, P. E. et al. Structural insights into the degradation of Mcl-1 induced by BH3 domains. *Proc. Natl Acad. Sci. USA* **104**, 6217–6222 (2007).
22. Wang, X. et al. Deletion of MCL-1 causes lethal cardiac failure and mitochondrial dysfunction. *Genes Dev.* **27**, 1351–1364 (2013).
23. Rasmussen, M. L. et al. MCL-1 inhibition by selective BH3 mimetics disrupts mitochondrial dynamics causing loss of viability and functionality of human cardiomyocytes. *iScience* **23**, 101015 (2020).
24. Janssen, J. et al. Hypothermic and cryogenic preservation of cardiac tissue-engineered constructs. *Biomater. Sci.* **12**, 3866–3881 (2024).
25. Pegram, H. J. et al. Tumor-targeted T cells modified to secrete IL-12 eradicate systemic tumors without need for prior conditioning. *Blood* **119**, 4133–4141 (2012).
26. Hu, B. et al. Augmentation of antitumor immunity by human and mouse CAR T cells secreting IL-18. *Cell Rep.* **20**, 3025–3033 (2017).
27. Kerkar, S. P. et al. Tumor-specific CD8+ T cells expressing interleukin-12 eradicate established cancers in lymphodepleted hosts. *Cancer Res.* **70**, 6725–6734 (2010).
28. Chmielewski, M. et al. IL-12 release by engineered T cells expressing chimeric antigen receptors can effectively Muster an antigen-independent macrophage response on tumor cells that have shut down tumor antigen expression. *Cancer Res.* **71**, 5697–5706 (2011).
29. Tang, L. et al. Arming CAR T cells with cytokines and more: Innovations in the fourth-generation CAR-T development. *Mol. Ther.* **31**, 3146–3162 (2023).

30. Woodsworth, D. J. et al. Targeted cell-to-cell delivery of protein payloads via the granzyme-perforin pathway. *Mol. Ther. Methods Clin. Dev.* **7**, 132–145 (2017).
31. Peperzak, V. et al. Mcl-1 is essential for the survival of plasma cells. *Nat. Immunol.* **14**, 290–297 (2013).
32. Vikstrom, I. et al. Mcl-1 is essential for germinal center formation and B cell memory. *Science* **330**, 1095–1099 (2010).
33. Opferman, J. T. et al. Obligate role of anti-apoptotic MCL-1 in the survival of hematopoietic stem cells. *Science* **307**, 1101–1104 (2005).
34. Opferman, J. T. et al. Development and maintenance of B and T lymphocytes requires antiapoptotic MCL-1. *Nature* **426**, 671–676 (2003).
35. Rinkenberger, J. L., Horning, S., Klocke, B., Roth, K. & Korsmeyer, S. J. Mcl-1 deficiency results in peri-implantation embryonic lethality. *Genes Dev.* **14**, 23–27 (2000).
36. Tantawy, S. I., Timofeeva, N., Sarkar, A. & Gandhi, V. Targeting MCL-1 protein to treat cancer: opportunities and challenges. *Front. Oncol.* **13**, 1226289 (2023).
37. Gardner, T. J. et al. Engineering CAR T cells to activate small-molecule drugs in situ. *Nat. Chem. Biol.* **18**, 216–225 (2022).
38. Marco-Malina, V. et al. Redirecting αβ T cells against cancer cells by transfer of a broadly tumor-reactive γδT-cell receptor. *Blood* **118**, 50–59 (2011).
39. Sun, F. et al. BCMA- and CST6-specific CAR T cells lyse multiple myeloma cells and suppress murine osteolytic lesions. *J. Clin. Invest.* **134**, e171396 (2024).
40. Hamad, S. et al. Generation of human induced pluripotent stem cell-derived cardiomyocytes in 2D monolayer and scalable 3D suspension bioreactor cultures with reduced batch-to-batch variations. *Theranostics* **9**, 7222–7238 (2019).
41. Sun, F. et al. Bispecific BCMA/CD24 CAR-T cells control multiple myeloma growth. *Nat. Commun.* **15**, 615 (2024).

## Acknowledgements

The authors thank the support facilities of the University Medical Center Utrecht. Synthetic NOXA and NOXA-TAMRA were kindly provided by Prof. dr. H. Ovaa, Department Cell and Chemical Biology, Leiden University Medical Centre, Leiden, The Netherlands. The authors would like to gratefully acknowledge Tomo Saric (Uniklinik Koln) for providing the human iPSC lines. This work was financially supported by research grants from the Dutch Cancer Foundation (KWF)/Alpe d'HuZes Foundation (11270, 13058, and 15595 to V.P., and 14459 to M.C.). The funding agency played no role in the design, reviewing, or writing of the manuscript.

## Author contributions

T.K., M.C., and V.P. designed the research; T.K., M.C., R.G.T., D.R.B., J.J., B.M., A.S., C.P., S.H., A.D.M., W.B., D.M.T.B., S.K., and V.L.P. performed the experiments; T.K., M.C., R.G.T., D.R.B., J.J., A.S. and V.P. analyzed the results; T.K., M.C., R.G.T., D.R.B., J.J., B.M., A.S., C.P., W.B., D.M.T.B., S.K., S.N., N.B., J.K., A.v.M., M.C.M., Z.S., and V.P. contributed to interpretation and discussion; T.K., M.C., and V.P. wrote and revised the manuscript; M.C., J.P.G.S., S.N., N.B., J.K., A.v.M., M.C.M., Z.S., and V.P. supervised the study. All authors reviewed and approved the final manuscript.

## Competing interests

V.P. received royalty payments related to venetoclax. V.P., Z.S., and T.K. are inventors on a patent for improving cytotoxicity of gene engineered T and NK cells. M.C.M. received research funding from Beigene, Janssen Cilag, Speakers fee from Janssen Cilag, Siemens, and Pfizer, and Consultancy fee from Janssen Cilag, Pfizer, BMS, and Hospitality Janssen Cilag, Beigene, all paid to institution. Z.S. and J.K. are inventors on different patents for γδ T-cell receptor sequences, recognition mechanisms, and isolation strategies. J.K. is the founder and shareholder of Gadeta Founders BV. The remaining authors declare no competing interests.

## Additional information

**Supplementary information** The online version contains supplementary material available at https://doi.org/10.1038/s41467-025-59818-8.

**Correspondence** and requests for materials should be addressed to Victor Peperzak.

**Peer review information** *Nature Communications* thanks Karlo Perica and the other anonymous reviewer(s) for their contribution to the peer review of this work. A peer review file is available.